

EVALUATING THE MORPHOLOGY OF THE LOCAL INTERSTELLAR MEDIUM: USING NEW DATA TO DISTINGUISH BETWEEN MULTIPLE DISCRETE CLOUDS AND A CONTINUOUS MEDIUM*

SETH REDFIELD¹ AND JEFFREY L. LINSKY²

¹ Astronomy Department and Van Vleck Observatory, Wesleyan University, Middletown, CT 06459-0123, USA; sredfield@wesleyan.edu

² JILA, University of Colorado and NIST, Boulder, CO 80309-0440, USA; jlinsky@jila.colorado.edu

Received 2015 August 21; accepted 2015 September 5; published 2015 October 15

ABSTRACT

Ultraviolet and optical spectra of interstellar gas along the lines of sight to nearby stars have been interpreted by Redfield & Linsky and previous studies as a set of discrete warm, partially ionized clouds each with a different flow vector, temperature, and metal depletion. Recently, Gry & Jenkins proposed a fundamentally different model consisting of a single cloud with nonrigid flows filling space out to 9 pc from the Sun that they propose better describes the local ISM. Here we test these fundamentally different morphological models against the spatially unbiased Malamut et al. spectroscopic data set, and find that the multiple cloud morphology model provides a better fit to both the new and old data sets. The detection of three or more velocity components along the lines of sight to many nearby stars, the presence of nearby scattering screens, the observed thin elongated structures of warm interstellar gas, and the likely presence of strong interstellar magnetic fields also support the multiple cloud model. The detection and identification of intercloud gas and the measurement of neutral hydrogen density in clouds beyond the Local Interstellar Cloud could provide future morphological tests.

Key words: ISM: atoms – ISM: clouds – ISM: structure – line: profiles – ultraviolet: ISM – ultraviolet: stars

1. DEVELOPMENT OF MULTIPLE CLOUD MORPHOLOGIES

The interstellar medium plays a critical role in astrophysics as the interface between the creation of metals in stars and their eventual inclusion in the next generation of stars. A significant fraction of the mass of galaxies is interstellar gas and the accretion and loss of this gas play critical roles in galactic evolution (e.g., Kennicutt 1998). Studies of the physical processes, thermal structure, and dynamics of interstellar gas include theoretical models, numerical simulations, and extensive observational studies typically involving high-resolution spectra of ultraviolet absorption lines. The local interstellar medium (LISM), which exists in close proximity to the Sun (i.e., within 100 pc), is the closest and simplest sample of interstellar gas to study with high-sensitivity absorption line spectra. A significant advantage of using LISM observations to evaluate interstellar structures is the small number of traversed absorbers and high likelihood that the interstellar gas velocity structure along the line of sight will be resolved in a high-resolution stellar spectrum.

From an analysis of high-resolution Ti II $\lambda 3384$ absorption line spectra toward stars within 100 pc of the Sun, Crutcher (1982) found that warm gas in the LISM is moving coherently with a heliocentric velocity vector $(l_o, b_o, V_o) = (25^\circ, +10^\circ, -28 \text{ km s}^{-1})$. He noted that this flow is consistent with an expanding shell of gas accelerated by the hot stars and supernovae in the Sco-Cen Association, and that this interstellar wind flow could explain the velocity of resonantly scattered solar H I Ly α and He I resonance lines.

Further understanding of the morphology and kinematics of the LISM required more sensitive high-resolution spectra, in particular, using ultraviolet absorption lines of H I and D I Ly α ,

Mg II $\lambda 2796$, 2802, Fe II $\lambda 2600$, O I $\lambda 1302, 1304, 1306$, C II $\lambda 1334, 1335$, and many weaker transitions of neutral and singly ionized elements. These spectral lines are particularly useful because the ions are abundant in the ISM and the permitted transitions are from the highly populated ground states. Such data began to appear in quantity from the increasingly sensitive and higher resolution spectrographs on *Copernicus*, the *International Ultraviolet Explorer (IUE)*, the Goddard High Resolution Spectrograph (GHRS) instrument on the *Hubble Space Telescope (HST)*, and finally the Space Telescope Imaging Spectrograph (STIS) instrument on *HST*.

Using *Copernicus*, McClintock et al. (1978) was able to measure H I column densities and radial velocities of interstellar gas in the lines of sight toward eight G and K stars within 15 pc of the Sun supporting the model of uniform flow of neutral interstellar gas in the solar neighborhood. *IUE* spectra of the H I Ly α line toward many hot stars allowed Frisch & York (1983) to create maps of hydrogen column density, which show an asymmetrical structure with an $N(\text{H I})$ hole centered at $l \sim 225^\circ$, $b \sim -15^\circ$.

Analysis of high-resolution GHRS spectra of the nearby stars α Cen (Linsky & Wood 1996), Sirius (Lallement et al. 1994; Bertin et al. 1995), Procyon (Linsky et al. 1995), Capella (Linsky et al. 1993), and others provided accurate column densities, velocities, and nonthermal broadening parameters for these lines of sight by combining information from the saturated H I Ly α line, the thermally broadened but unsaturated D I Ly α line, and lines of heavy elements like Mg II and Fe II that reveal the velocity structure along the line of sight.

The next step in our understanding of the structure of partially ionized gas in the LISM was the recognition that individual comoving structures (called clouds) could be identified by the common space velocities of gas across large regions of the sky. Early efforts used Ca II observations (e.g., Lallement et al. 1986), although these cloud vectors were significantly revised with a larger sample of observations (Vallerga et al. 1993). Lallement & Bertin (1992), using

* Based on observations made with the NASA/ESA *Hubble Space Telescope*, obtained from the Data Archive at the Space Telescope Science Institute, which is operated by the Association of Universities for Research in Astronomy, Inc., under NASA contract NAS AR-09525.01A. These observations are associated with programs #11568.

essentially Ca II observations, and Lallement et al. (1995), using primarily high-resolution ultraviolet spectra, identified two clouds: the G cloud in the direction of the Galactic Center, and the Local Interstellar Cloud (LIC) centered in the opposite direction and likely containing the Sun on the basis of their projected velocity differences. Redfield & Linsky (2000) produced a three-dimensional map of the LIC on the basis of 16 lines of sight observed by GHRS, 13 lines of sight observed with the Ca II lines, and three lines of sight to hot white dwarfs observed by the *Extreme Ultraviolet Explorer* (EUVE). The accumulation of additional observations with the GHRS and STIS instruments on *HST* by Dring et al. (1997), Frisch et al. (2002), Redfield & Linsky (2002, 2004), and others were the basis for more detailed models of the LISM. Frisch et al. (2002) proposed a kinematic model with seven clouds based on 96 velocity components detected toward 60 stars.

Redfield & Linsky (2008, hereafter RL08) next developed a 15 cloud model of the LISM on the basis of 270 radial velocity measurements toward 157 stars located within 100 pc of the Sun. The assignment of individual velocity components to a cloud was based mainly on kinematics (i.e., the radial velocities are consistent to within the measurement errors of a common velocity vector for a number of targets distributed over a large region of the sky), although contiguity of the sight line coordinates was also a criterion. The shape of the clouds, which was drawn by eye to include the Galactic coordinates of the assigned targets, is subjective and has been refined over time (e.g., Malamut et al. 2014, hereafter M14) with the inclusion of new sight lines. Because of the close proximity of these clouds to the Sun, they typically subtend large angles on the sky. This provides leverage to measure the three-dimensional velocity vector from a sample of radial velocity measurements, and thereby to measure the transverse velocities of these clouds. Clouds at a greater distance, or with small linear sizes cannot be identified with this technique. The conditions for which a cloud can be identified are complex and hard to quantify, but the accuracy of the velocity vector can be estimated from the errors in its components (see Table 16 of RL08).

All of these warm partially ionized clouds, now called the complex of local interstellar clouds (CLIC), lie entirely or in part within 15 pc of the Sun because the nearest stars showing absorption by the gas in each cloud lie within this distance. Since all of these sight lines show absorption by partially ionized gas in these clouds or in not yet identified clouds, there is presently no direction in space where $\log N(\text{H I}) < 17.4$ toward an observed star. Comparison of the widths of absorption lines of a low-mass element (e.g., D) with high-mass elements (e.g., Fe and Mg) allowed Redfield & Linsky (2008) to infer the gas temperature of the LIC to be $T = 7500 \pm 1300$ K and the temperatures of the other clouds to lie in the range 3900 K (Blue) to 9900 K (Mic). Frisch (2009) and Frisch et al. (2011) noted that the inferred temperatures and nonthermal broadening parameters assume a Maxwell–Boltzmann distribution of velocities and mass-independent turbulence, both of which may not be valid in low density clouds.

Frisch (2009) concluded that the physical properties of the CLIC clouds are typical of warm partially ionized gas observed elsewhere in the solar neighborhood on the basis of temperature, velocity, composition, ionization, and magnetic field properties. In particular, the ionization equilibrium of the CLIC gas is consistent with the local EUV radiation field

(Slavin & Frisch 2008). The recent comprehensive review of the interstellar medium surrounding the Sun by Frisch et al. (2011) describes our present understanding of the Galactic environment of the LISM, the role of outflowing gas from the Sco-Cen association as a driver for the CLIC kinematics, the interstellar radiation field, ionization, and depletion of metals in the gas, kinematics of the gas, and the interstellar magnetic field.

2. AN ALTERNATIVE MODEL FOR THE CLIC MORPHOLOGY

Gry & Jenkins (2014, hereafter GJ14) have proposed a fundamentally different morphological model for the warm interstellar gas located near the Sun in which all of the space within about 9 pc of the Sun consists of a single continuous cloud with a nonrigid flow and a gradient in metal depletion properties. They fit the Redfield & Linsky (2002) Mg II and Fe II radial velocity data set with a nonrigid flow that is differentially decelerated in the direction of motion and expanding in directions perpendicular to the flow. In their Single Local Cloud model, the flow speed and direction near the Sun is consistent with the speed and direction of interstellar helium flowing into the heliosphere as measured by the *Interstellar Boundary Explorer* (IBEX) and *Ulysses* satellites. They found that their single local cloud model fits nearly all of the Mg II and Fe II velocity components that RL08 assigned to the LIC, G, NGP, Blue, Leo, Aur, and Cet clouds. If the mean neutral hydrogen density is 0.055 cm^{-3} , as inferred from the hydrogen column densities and distances of nearby stars, then their single cloud model fills all of the space out to roughly 9 pc from the Sun. GJ14 also found that another set of velocity components that RL08 had assigned to the Hyades and Mic clouds and including many of the previously unassigned velocity components, could be fit by a second vector that they called the Cetus Ripple, which may be a signature of a shock front inside of the local cloud. They speculated that the remaining unassigned velocity components are also perturbations located inside of the local cloud.

3. A CRITICAL TEST OF THE TWO MORPHOLOGICAL MODELS

Both the GJ14 and RL08 models were constructed to fit the Redfield & Linsky (2002) data set of Mg II and Fe II absorption line radial velocities, although the RL08 model was constructed to also fit radial velocities for other lines of sight measured from Ca II line spectra. A critical test of the viability of both models is, therefore, to determine how accurately each model predicts the radial velocities of a new data set with targets randomly distributed in Galactic coordinates.

M14 obtained high-resolution STIS E230H spectra of the Mg II, Fe II, and Mn II lines in the 2580–2805 Å spectral region for stars that previously had only 1200–1700 Å spectra. This new data set consists of 76 velocity components measured in the lines of sight toward 34 stars. To be consistent with the RL02 sample, we limit our analysis to stars within 100 pc, and therefore only used 32 of the 34 sight lines from this sample. The data were obtained in the SNAPshot observing mode—designed to provide short (typically one spacecraft orbit) observations to fill gaps in the *HST* schedule. Since the observed targets were selected by the *HST* schedulers from a large list of stars distributed across the sky, the observed targets

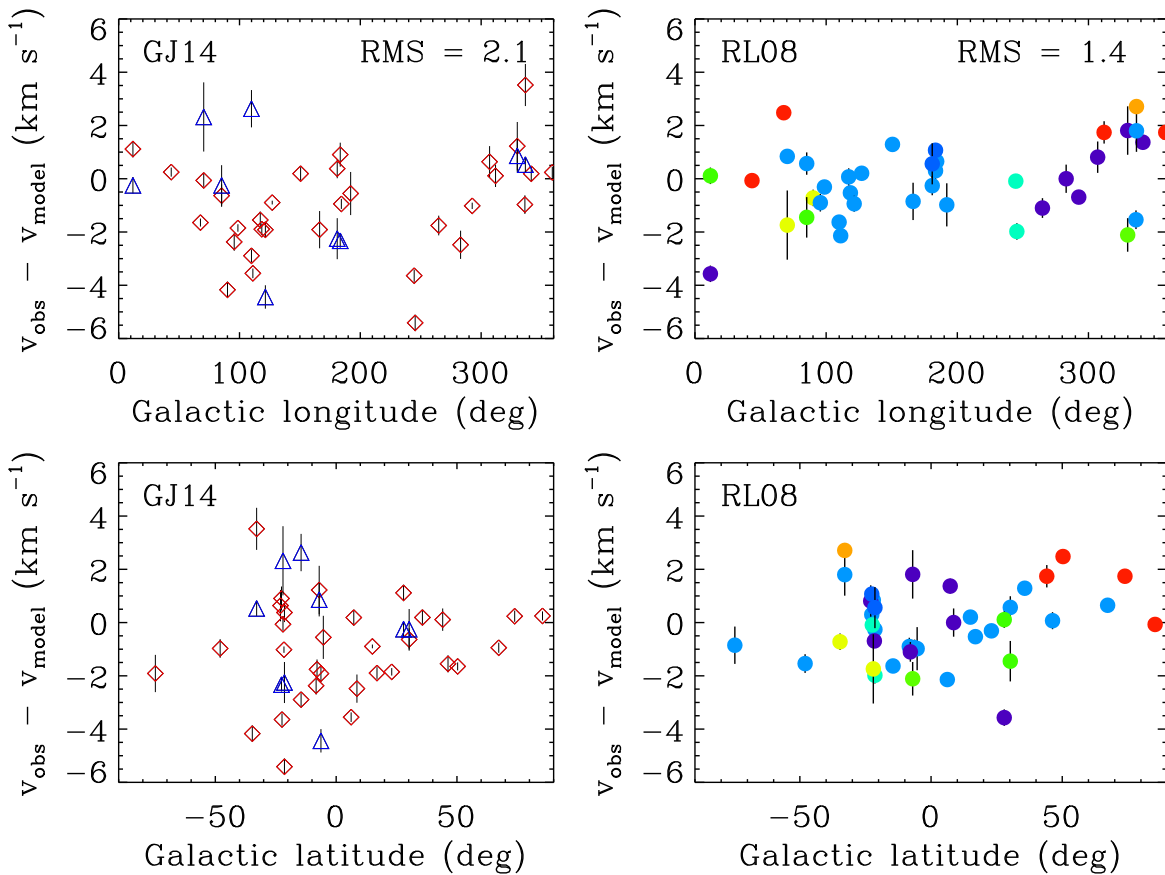


Figure 1. Comparison of the velocity offsets (observed minus model prediction) for the **M14** data set. Left panels use the **GJ14** model (red for Component 1 and blue for the Cetus Ripple component). Right panels use the **RL08** model (the color coding is by cloud structure, which is dominated by the LIC (blue), G Cloud (violet), and NGP Cloud (red)). The root mean scatter (RMS) is given in the top right corner, and is a factor of 1.5 lower for the **RL08** model than the **GJ14** model.

are, in effect, randomly distributed in Galactic coordinates as shown in Figure 1 in **M14**. The **M14** data set, therefore, provides us with an appropriate basis for testing the two models.

We will evaluate how well the **GJ14** and the **RL08** models fit the new data and utilize some statistical tests to make quantitative comparisons; however, statistical tests have their limitations as the fitting parameters for the two models are very different and could lead to possible systematic errors. Figure 1 compares the observed minus predicted radial velocities for the two models as a function of Galactic longitude and latitude using the **M14** data set. The left panels separate by color the predicted velocities for the Local Cloud (32 measurements) and Cetus Ripple (9 measurements) using the procedure proposed by **GJ14**. The right panels make a similar comparison for the exact same set of velocity components, except using instead the **RL08** model for their suite of discrete clouds. Note that two components associated with the Cetus Ripple by **GJ14** are not identified with a known cloud in the **RL08** model resulting in $32 + 9 = 41$ total points in the **GJ14** comparison and $32 + 7 = 39$ points in the **RL08** comparison. For the latter comparison, we use a weighted mean velocity based on all available LISM measurements, which for the **M14** sample is primarily Mg II and Fe II. This mitigates systematic errors that can arise from using a single ion (e.g., due to saturation or wavelength calibration issues).

Figure 2 shows a similar set of comparisons, but now using the **RL08** data set. This data set includes observations tabulated

in Redfield & Linsky (2002, 2004), totaling ~ 80 sight lines. The **GJ14** interpretation of the data results in 80 Local Cloud and 36 Cetus Ripple assignments, totally 116 components. The **RL08** interpretation of the data results in 122 cloud identifications. This comparison using this full sample is not as clear of a test of the two morphological models because both models were constructed to fit these data (together with some Ca II data for the **RL08** model). Nevertheless, this second comparison is useful as a confirmation of the results of the first comparison.

As shown in Figures 1 and 2, the **RL08** model clearly provides a much tighter fit to both the **M14** and **RL08** data sets. The root mean square (rms) scatter for the **RL08** model is a factor of 1.5 or two times smaller than for the **GJ14** model: 1.4 versus 2.1 for the **M14** data set and 0.77 versus 1.5 for the **RL08** data set. However, the **RL08** model has 45 free parameters (3 for each of the 15 clouds), versus the 8 free parameters in the **GJ14** model. For the **GJ14** model, there are 3 parameters for the Local Cloud velocity vector, an additional 3 for the deformation (direction and magnitude), and 2 for the Cetus Ripple, which is just an offset and range around that offset. An F -test shows that even with more free parameters, the **RL08** model is statistically preferred. If we look at the entire data set, that is data included in **RL08** and **M14**, the **GJ14** model has a reduced χ^2_ν of 49.5, with 149 degrees of freedom (157–8), whereas the *same* 157 components in the **RL08** model has a reduced χ^2_ν of 30.4, with 112 degrees of freedom (157–45). There is a 0.4% probability that such a dramatic difference in the ratio of χ^2 could be the result of a random set

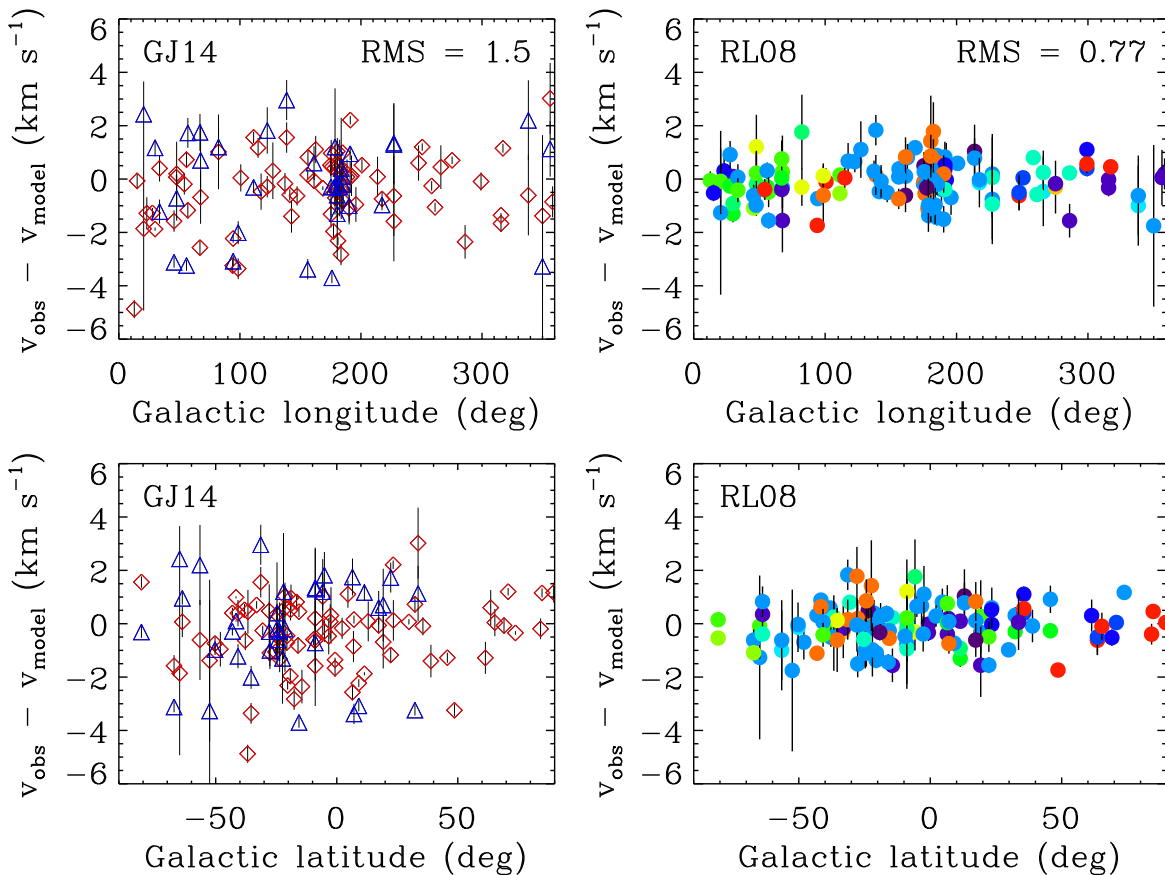


Figure 2. Comparison of the velocity offsets (observed minus model prediction) for the **RL08** data set. Left panels use the **GJ14** model (red for Component 1 and blue for the Cetus Ripple component). Right panels use the **RL08** model (the color coding is by cloud structure, which is dominated by the LIC (blue), Hyades Cloud (orange), G Cloud (violet), Mic Cloud (green), Blue Cloud (dark blue), and NGP Cloud (red)). The rms scatter is given in the top right corner, and is a factor of two lower for the **RL08** model than the **GJ14** model.

of data as compared to the true model, even taking into account the higher number of parameters for the **RL08** model (Bevington & Robinson 1992). Note that the χ^2 calculations above use the individual, published velocity errors, whereas **GJ14** implemented a velocity error floor of 1.1 km s^{-1} . If we make the same assumption regarding the velocity errors, the reduced χ^2_ν values become 2.30 and 0.92 for the **GJ14** model and **RL08** model, respectively. However, the basic conclusion remains the same, that the difference in the quality of fit between the two models is significant.

Of the 210 velocity components (147 from the **RL08** data sample and 63 from the **M14** sample, which excludes those $>100 \text{ pc}$ and a component identified with absorption from a circumstellar disk), the **RL08** model is able to successfully fit 175 (83%), whereas the **GJ14** model fits 157 (75%). While the **GJ14** model must have a Local Cloud component along every sight line, in practice, essentially all sight lines have at least one successfully assigned component in the **RL08** model. On the other hand, the **GJ14** model is unable to account for sight lines with more than two absorption components (Local Cloud and Cetus Ripple), whereas the **RL08** model can account for them with several clouds along the line of sight. Although the velocity component assignment percentages are similar between the two models, the predictive power of the **RL08** model is much better than the **GJ14** model when tested against the **M14** data set and the entire data set as a whole.

For all 34 stars observed and analyzed by **M14**, the **RL08** kinematic model predicts 40 absorbers along the lines of sight.

All 40 radial velocity predictions are successfully detected in the **M14** sample to within measurement uncertainty (i.e., within $\sim 3\sigma$). The **RL08** kinematic model also accurately predicts the observed radial velocities for 18 absorbers along sight lines lying within 20° of a cloud boundary. The **RL08** model clouds have the condition of being contiguous, and have a spatial extent (as does the Cetus Ripple in the **GJ14** model). Given the relative sparseness of the sample, the precise cloud morphologies are not necessarily well constrained, but will be refined as new data is made available as long as the cloud boundary remains contiguous. In their high-resolution STIS spectra of three early B stars located about 70 pc from the Sun, Welsh & Lallement (2010) also found that 8 out of 11 velocity components for these lines of sight are consistent with the predicted velocities of six clouds in the **RL08** kinematic model. The 40 out of 40 success rate in ascribing **M14** radial velocities to clouds confirms the robustness of the **RL08** model, although any model consisting of rigid flow structures is an approximation to what is likely a more complex flow pattern that could include rotation in addition to nonrigid translation terms. It is likely that a more realistic description of the CLIC kinematics lies somewhere between the two extreme morphologies.

4. DISCUSSION: WHICH MORPHOLOGICAL MODEL IS MORE REALISTIC AND WHY IS THIS IMPORTANT?

Whether the warm partially ionized interstellar gas located within a few parsecs of the Sun has a continuous or a discrete

multicloud morphology is important because the morphology can provide important clues concerning the physical properties of the gas and its evolution.

The presence of discrete clouds requires a structuring agent that could be ionizing radiation from an assorted distribution of different hot stars shielded by clouds in some directions, inhomogeneous magnetic fields, shock waves, or thermal instabilities. If the warm gas is indeed structured into discrete separated clouds, then there must be gas located between the clouds that is difficult to detect in spectral lines of hydrogen and singly ionized metals. This intercloud gas has not been unambiguously characterized perhaps because it is very hot (roughly 10^6 K) as originally suggested by the observed diffuse soft X-ray emission (see Cox 2005), and recently confirmed by Galeazzi et al. (2014). However, a significant contribution to this soft X-ray emission results from charge-exchange emission inside of the heliosphere (Snowden et al. 1994; Koutroumpa 2012). Components of the intercloud medium could be comprised of highly ionized recombining gas (Welsh & Shelton 2009) or Stromgren sphere 10^4 K ionized hydrogen gas surrounding nearby hot stars like Sirius B (Tat & Terzian 1999). An advantage of the continuous cloud morphology model is that it does not require interstitial gas and is therefore consistent with its nondetection, whereas discrete detached multicloud models require the presence of such gas and, if/when detected, the properties of this gas will provide insight into the energy balance of the CLIC.

Whether the warm cloud gas fills a small fraction or essentially all of the volume within about 9 pc of the Sun depends upon the neutral hydrogen gas density. If $n(\text{H I}) \approx 0.20 \text{ cm}^{-3}$ is typical for the warm gas in nearby clouds, as Slavin & Frisch (2008) find for the LIC, then the warm partially ionized clouds fill a small fraction of nearby space. If, on the other hand, $n(\text{H I}) \approx 0.055 \text{ cm}^{-3}$, as suggested by GJ14, then the warm gas fills all of the nearby space and there is no interstitial gas within about 9 pc of the Sun.

Gry & Jenkins (2014) note that if the LISM is comprised of discrete clouds and the filling factor is low, it is likely that sight lines could be found that do not traverse any warm gas and, therefore, show no LISM absorption. However, every sight line analyzed so far shows detected interstellar absorption with $\log N(\text{H I}) > 17.4$. Redfield & Linsky (2008) reported a filling factor of 5.5%–19% for their suite of 15 clouds, but this calculation assumed the maximum possible spacing of the clouds (limited to the closest stars that showed absorption for a particular cloud) and the placement of the clouds within 15 pc of the Sun. Also, Welsh & Lallement (2010) argued that the clouds are all located within 10 pc because there is little warm gas between 10 pc and the 70 pc location of their targets. In order to explore the question of why there are not gaps in H I absorption, we recomputed the suite of simulations described in Redfield & Linsky (2008) while keeping track of the probability of any given sight line avoiding all simulated clouds. Our objective was to find an upper limit to the total volume enclosing the LISM clouds that predicts that essentially all lines of sight to nearby stars have observable H I absorption. We made several simplifying assumptions in this analysis and our conclusions are based on a statistical sample of simulated LISM configurations. A more accurate estimate would require a full three-dimensional model of the LISM based on the entire data set. We find that if all the clouds are located within 7 pc of the Sun, the filling factor ranges from 55% to 100% and there is

a $\sim 99.6\%$ probability that all sight lines will traverse at least one absorbing cloud (using the original 15 pc limit, this probability is $\sim 65\%$). We conclude that if the 15 clouds in the RL08 model are located within 7 pc, there should be few or no gaps in the projection of these clouds on the sky and no sight lines to nearby stars with undetected H I absorption. Note that this conclusion is strongly dependent on the number of very nearby stars (e.g., < 5 pc), and an observational campaign to expand this sample could be a powerful discriminant between these two models. While both the GJ14 and RL08 models largely fill the immediate interstellar space surrounding the Sun, the kinematic properties of the two models are quite distinct, which may hold clues regarding the origin and evolution of this material.

There is evidence that the interstellar magnetic field strength immediately surrounding the heliosphere lies in the range 2.7–5 μG (Frisch et al. 2011). Since the beginning of 2013, the *Voyager 1* spacecraft has been making in situ measurements of the interstellar magnetic field strength outside of the termination shock with a mean value of $4.64 \pm 0.09 \mu\text{G}$ and nearly constant orientation very different from that of the solar magnetic field inside of the heliosheath (Gurnett et al. 2013; Burlaga & Ness 2014a, 2014b). Although the measured magnetic field likely refers to the field draped around the heliopause, which may be compressed relative to the undisturbed field far away from the Sun, *Voyager 1* has provided us with the best available estimate of the interstellar magnetic field strength near the Sun. Since equipartition between magnetic and thermal energy is about 2.7 μG in the LIC, the *Voyager 1* magnetic field strength measurement indicates that strong interstellar magnetic fields are present near the Sun and could, therefore, control the structure of discrete clouds. The thin elongated structures of several clouds identified by RL08 (Aur, Cet, Mic, and perhaps others) are consistent with confinement by elongated parsec scale magnetic fields.

Large-amplitude intraday and annual scintillations of some well monitored, unresolved quasars at radio wavelengths indicate turbulent-scattering screens in the CLIC. Linsky et al. (2008) showed that the variability of three well-studied quasars (B1257-326, B1519-273, and J1819+385) can be understood as produced by the Earth's orbital motion through the diffraction pattern of scattering screens located within 7 pc of the Sun. The lines of sight to these quasars pass close to the outer edges of two or more adjacent or perhaps colliding clouds. The shear of the different cloud velocities and the likely higher ionization of the gas at the cloud edges due to external ionizing radiation or thermal conduction from hot surrounding gas could produce the turbulent ionized plasma and the inhomogeneous index of refraction properties of scattering screens. The transverse velocities measured for these scintillation screens match very well with a cloud in their line of sight for the RL08 model but poorly for gas at the Local Standard of Rest. The nonrigid structure of the GJ14 model is consistent with a scattering screen in the J1819+385 sight line, but cannot explain the scattering screens for the other two sight lines. The existence of nearby scattering screens provides additional evidence that isolated warm clouds with ionized edges rather than a single cloud even with a nonrigid velocity structure can more naturally explain the complexity observed in the LISM velocity structure.

Another test of whether or not warm partially ionized gas is confined in identifiable clouds, would be the observation of absorption by high ionization species located near the outer boundaries of clouds produced by either thermal conduction from surrounding hot gas or ionization by the extreme ultraviolet radiation from ϵ CMA and other sources. Searches for O VI $\lambda 1032$ absorption (e.g., Savage & Lehner 2006) led to detections in hot white dwarf photospheres but not in the interstellar medium. In their summary of searches for lower stages of ionization in the LISM, Welsh et al. (2010) found that the only clear example is interstellar C IV absorption in the line of sight to the B2Ve star HD 158427 located at a distance of ~ 74 pc inside of the Local Cavity. This detection is very interesting because the observed radial velocity, -24.3 ± 2.0 km s $^{-1}$, is consistent with the projected radial velocities of both the G and Aquila clouds and the line of sight to HD 158427 is tangential to the edges of both clouds as shown in RL08. This is the most favorable geometry for the detection of weak absorption because of the long line of sight through the cloud edges.

5. CONCLUSIONS

The M14 database of interstellar radial velocities provides an unbiased test of the robustness of two fundamentally different morphological models of the interstellar medium within a few parsecs of the Sun. Both the multiple discrete cloud model proposed by RL08, for which each cloud has a rigid flow vector, and the single local cloud model with nonrigid flows proposed by GJ14 are approximations of what is likely a more complex kinematic and morphological structure. Nevertheless, it is instructive and important to test the predictive power of both models. We find that the RL08 model fits the new velocity data significantly better than the GJ14 model and provides a natural way of explaining the observed multiple velocity components along the lines of sight to many nearby stars. Also, the likely presence of strong magnetic fields and scattering screens in the CLIC are arguments for the presence of multiple clouds that do not entirely fill nearby space, although a close packing of clouds is likely, resulting in a high filling factor and a low probability of a sight line displaying no observable LISM absorption. Important future tests of the CLIC morphology would be the detection and identification of interstitial gas, if it is present, and the measurement of neutral hydrogen densities far away from the heliosphere. A more densely sampled observational data set, particularly comprised of very close stars (e.g., < 5 pc), would also provide definitive tests between smoothly varying deformed kinematics of a continuous medium and the more striking variations that would arise in a suite of discrete absorbers. We encourage future model development and testing to better understand the physical properties and evolution of the interstellar medium close to the solar neighborhood.

We acknowledge support through NASA *HST* grant GO-11568 from the Space Telescope Science Institute, which is operated by the Association of Universities for Research in Astronomy, Inc. for NASA under contract NAS5-26555. We thank Drs. Cecile Gry and Edward Jenkins for their careful reading and in-depth comments concerning an earlier version of this paper that guided us in completing it. We appreciate the expeditious and insightful review by the referee.

Facility: *HST* (GHRS, STIS).

REFERENCES

- Bertin, P., Vidal-Madjar, A., Lallement, R., Ferlet, R., & Lemoine, M. 1995, *A&A*, **302**, 889
- Bevington, P. R., & Robinson, D. K. 1992, *Data Reduction and Error Analysis for the Physical Sciences* (2nd ed.; New York: McGraw-Hill)
- Burlaga, L. F., & Ness, N. F. 2014a, *ApJ*, **784**, 146
- Burlaga, L. F., & Ness, N. F. 2014b, *ApJL*, **795**, L19
- Cox, D. P. 2005, *ARA&A*, **43**, 337
- Crutcher, R. M. 1982, *ApJ*, **254**, 82
- Dring, A. R., Linsky, J. L., Murthy, J., et al. 1997, *ApJ*, **488**, 760
- Frisch, P. C. 2009, *SSRv*, **143**, 191
- Frisch, P. C., Grodnicki, L., & Welty, D. E. 2002, *ApJ*, **574**, 834
- Frisch, P. C., Redfield, S., & Slavin, J. D. 2011, *ARA&A*, **49**, 237
- Frisch, P. C., & York, D. J. 1983, *ApJL*, **271**, L59
- Galeazzi, M., Chiao, M., Collier, M. R., et al. 2014, *Natur*, **512**, 171
- Gry, C., & Jenkins, E. B. 2014, *A&A*, **567**, A58
- Gurnett, D. A., Kurth, W. S., Burlaga, L. F., & Ness, N. F. 2013, *Sci*, **341**, 1489
- Kennicutt, R. C. 1998, *ApJ*, **498**, 541
- Koutroumpa, D. 2012, *AN*, **333**, 341
- Lallement, R., & Bertin, P. 1992, *A&A*, **266**, 479
- Lallement, R., Bertin, P., Ferlet, R., Vidal-Madjar, A., & Bertaux, J. L. 1994, *A&A*, **286**, 898
- Lallement, R., Ferlet, R., Lagrange, A. M., Lemoine, M., & Vidal-Madjar, A. 1995, *A&A*, **304**, 461
- Lallement, R., Vidal-Madjar, A., & Ferlet, R. 1986, *A&A*, **168**, 225
- Linsky, J. L., Brown, A., Gayley, K., et al. 1993, *ApJ*, **402**, 694
- Linsky, J. L., Diplas, A., Wood, B. E., et al. 1995, *ApJ*, **451**, 335
- Linsky, J. L., Rickett, B. J., & Redfield, S. 2008, *ApJ*, **675**, 413
- Linsky, J. L., & Wood, B. E. 1996, *ApJ*, **463**, 254
- Malamut, C., Redfield, S., Linsky, J. L., Wood, B. E., & Ayres, T. R. 2014, *ApJ*, **787**, 75
- McClintock, W., Henry, R. C., Linsky, J. L., & Moos, H. W. 1978, *ApJ*, **225**, 465
- Redfield, S., & Linsky, J. L. 2000, *ApJ*, **534**, 825
- Redfield, S., & Linsky, J. L. 2002, *ApJS*, **139**, 439
- Redfield, S., & Linsky, J. L. 2004, *ApJ*, **602**, 776
- Redfield, S., & Linsky, J. L. 2008, *ApJ*, **673**, 283
- Savage, B., & Lehner, N. 2006, *ApJS*, **162**, 134
- Slavin, J. D., & Frisch, P. C. 2008, *A&A*, **491**, 53
- Snowden, S. L., McCammon, D., Burrows, D. N., & Mendenhall, J. A. 1994, *ApJ*, **424**, 714
- Tat, H. T., & Terzian, Y. 1999, *PASP*, **111**, 1258
- Vallerga, J. V., Vedder, P. W., Craig, N., & Welsh, B. Y. 1993, *ApJ*, **411**, 729
- Welsh, B. Y., & Lallement, R. 2010, *AJ*, **122**, 1320
- Welsh, B. Y., & Shelton, R. L. 2009, *Ap&SS*, **323**, 1
- Welsh, B. Y., Wheatley, J., Siegmund, O. H. W., & Lallement, R. 2010, *ApJL*, **712**, L199